Computation & theory

Structural, mechanical and electronic properties of hafnium borides: a first principle study

Hai-Sheng Lin[1], Cheng-Yong Wang[1,*] , Mohamed-Abdou Djouadi[2], Tong-Chun Kuang[3], and Hua-Feng Dong[4]

[1] *School of Electromechanical Engineering, Guangdong University of Technology, Guangzhou 510006, China*
[2] *Institut Des Matériaux Jean Rouxel, Université de Nantes, CNRS, 44322 Nantes Cedex 3, France*
[3] *School of Materials Science and Engineering, South China University of Technology, Guangzhou 510641, China*
[4] *School of Physics and Optoelectronic Engineering, Guangdong University of Technology, Guangzhou 510006, China*

ABSTRACT

Transition metal boride, especially the hafnium boride Hf-B, is important and attractive to various applications. Understanding the correlations of material structure to mechanical properties is crucial for designing and synthesizing Hf-B compounds. In this paper, potential structures of the Hf-B system are systematically explored, and their hardness-enhancing and strength failure mechanisms are revealed through first-principle calculations. The results show that hardness of the compounds is estimated to be hard or superhard and is found to be sensitive to the B concentrations and types of sandwich-like structures. For Hf-B with sandwiches II structure, the bulk modulus, shear modulus, Young's modulus, hardness and ideal strength have linear relationship with B concentrations. Strong boron covalent bonding leads to the superhardness of Hf-B compounds with sandwiches I structure and $B/(Hf + B) > 0.66$. The newly predicted structure $C2$-HfB_6 is estimated to have a superhardness of up to 50 GPa. When applying large deformation, the weakest ideal strengths of the calculated compounds are lower than 20 GPa, due to the breaking of specific Hf-B bonds and the shifting of specific angles of B atoms.

Introduction

Transition metal boride (TMB) compounds are potential superhard materials because of the high electron concentration in transition metal and the formation of short covalent bond by the light element

B [1]. TM-B compounds are good candidate for novel superhard materials to replace diamond [2] and c-BN [3], which are synthesized at high pressure. In addition to high hardness, TM-B has unique features like high melting temperature, high chemical stability, and high thermal conductivity. Therefore, TM-B

 Springer

compounds have attracted growing attention recently. More and more previously unknown TM-B compounds have been discovered. For example, based on ab initio evolutionary methods, some TM-B systems, namely V-B [4], Fe-B [5], Ti-B [6], W-B [7], Mn-B [8], Mo-B [9], et al., are theoretically investigated. AlB$_2$- and ReB$_2$-type TMB$_2$ [10–12] are two most well-known structures. Besides, CrB-type, Ta$_5$B$_6$-type, Ta$_3$B$_4$-type and V$_2$B$_3$-type TM-B compounds are also common and intensively studied for many TM-B systems [13–15] and proved to be dynamical and mechanically stable.

Hafnium and its compounds have become critical materials used in nuclear reactors and the aerospace industry [16]. HfB$_2$, known as ultra-high-temperature ceramic (UHTC), is now frequently used in hypersonic applications due to its special features such as high thermal conductivity (105 Wm^{-1} K^{-1}), high melting temperature (3300 °C), large bulk hardness, low electrical resistivity and high chemical stability [17, 18]. In addition, HfB$_2$ compounds were found to possess the highest chemical stability among several 3d, 4d and 5d TMB$_2$ compounds [11] and superior oxidation resistance [19]. However, most of the research studies on HfB$_2$ compounds focus on the structure, preparation and performance of HfB$_2$-SiC composite materials used as a UHTC in the aerospace industry. There is many research study on Hf-N (i.e., HfN [20] and Hf$_3$N$_4$ [21]), Hf-C (i.e., HfC [22] and HfTaC$_2$ [23]) and other TM-B systems (i.e., TiB$_2$ [24] and WB$_2$ [25]). These compounds have been widely used in cutting tools, batteries, aerospace, and nuclear reactions. However, for Hf-B compounds, only $P6/mmm$-HfB$_2$, HfB [26] and Fm$\overline{3}$m-HfB$_{12}$ [27, 28] were reported to be experimentally synthesized, and the existing structures of HfB are disputable [29].

In recent years, there are more and more reports on the theoretical calculation of the structure of Hf-B compounds, such as $I4/mcm$-Hf$_2$B [30], Fm-$3m$-HfB [30], CrB-HfB [13, 31], $C2/m$-HfB$_3$ [32], $Cmcm$-HfB$_4$ [33], $C2/m$-HfB$_5$, $Pmmn$-HfB$_5$ [34], Amm2-HfB$_6$ [34], et al. In the theoretical calculation of Congwei Xie et al., it was found that $P6/mmm$-HfB$_2$ is the only thermodynamically stable phase at zero temperature and zero pressure [34]. However, it is necessary to conduct a more comprehensive study on the structure of Hf-B compounds and classify the structure types, in order to provide theoretical support for their

properties and further practical engineering applications.

There are also related reports on the calculation of mechanical properties of Hf-B compounds. In the theoretical calculation of Ta_3B_4-type M$_3$B$_4$ (M = Ti, V, Cr, Zr, Nb, Mo, Hf, Ta), the Poisson's ratio has the order of Hf$_3$B$_4$ < Ta$_3$B$_4$ < W$_3$B$_4$, suggesting that the more valence electrons, the better of ductility. Many factors, including boron concentration, phase structure, chemical bonding states, greatly influence the hardness of TM-B compounds. TM-B with high boron concentration may be expected to have outperforming mechanical properties, due to strong covalence bonding and covalent bonds to metals [35–39]. Some boron-rich Hf-B compounds including $C2/m$-HfB$_3$ [32], $Cmcm$-HfB$_4$ [33], and $C2/m$-HfB$_5$ [34] have been theoretically reported recently and found to have superhardness, suggesting that there may existing more Hf-B compounds with attractive properties. It is reported that both of the boron concentration and the boron sublattice are important for the mechanical properties of hafnium borides [34]. However, study of the change of elastic properties and strength failure mechanisms under different Hf-B compounds structure is lack.

This work systematically studies Hf-B compounds with variable compositions using the ab initio evolutionary algorithm at both ambient and high (50 GPa) pressure. The present calculated Hf-B compounds were demonstrated to be thermodynamically and mechanically stable. Further, the calculated Hf-B compounds were divided into two different sandwiches structures. The mechanical properties of Hf-B with different structure types were comprehensively studied, including the bulk modulus, shear modulus, Young's modulus, hardness and ideal strength. Moreover, the hardness-enhancing and strength failure mechanisms of Hf-B compounds were obtained.

Computation method

To search for the potential crystal structure of the Hf-B system, we performed the variable-composition calculation to find the stable phase and nearly stable compositions using the evolutionary algorithm implemented in the USPEX code [40–43]. A maximum of 30 atoms (Hf plus B) in a primitive cell were set during the search. The initial population

including 120 structures was produced randomly, with all the subsequent generations consisting of 100 structures produced by heredity (40%), random structure generator (20%), softmutation (20%), and transmutation (20%).

For the candidate new structures, structure relaxation and energy calculations were performed using density-functional theory (DFT) with the projector-augmented wave (PAW) method [44] as implemented in the VASP code [45], which is a plane-wave code for ab initio density-functional calculations. The electronic configurations of $50p^65d^26s^2$ and $2s^22p^1$ were adopted for Hf and B, respectively. Generalized gradient approximation (GGA) [46] of Perdew–Burke–Ernzerhof (PBE) exchange–correlation function [47] was performed. The plane-wave kinetic energy cutoff was set to be 600 eV and the k-point mesh resolution in reciprocal space is less than $2\pi \times 0.04$ Å^{-1}. The change of forces per atom is less than 0.001 eV/Å in geometry relaxation. All the parameters were carefully evaluated to ensure that the self-consistent total energies converged to within 1×10^{-6} eV/atom. The formation enthalpies of compounds Hf_xB_y were calculated by $\triangle H$ (per atom) = $\{H(Hf_xB_y) - [xH(Hf) + yH(B)]\}/(x + y)$. In this formula, $H(Hf_xB_y)$, $H(Hf)$ and $H(B)$ are enthalpies of Hf_xB_y (per formula), stable phases of hex-Hf and α-B (per atom), respectively, at a given pressure.

The elastic constants C_{ij} were calculated by the strain–stress method [48, 49], based on a well-known tensorial form of Hooke's law describing the linear dependency of stress components and the applied strain under a slight deformation. The bulk modulus B, shear modulus G, Young's modulus Y and Poisson's ratio v were extracted from the elastic constants. B and G can be estimated by the Voigt-Reuss-Hill method for polycrystalline materials [50],

$$B = (B_v + B_R)/2 \tag{1}$$

$$G = (G_V + G_R)/2 \tag{2}$$

$$E = 9BG/(3B + G) \tag{3}$$

$$v = (3B - 2G)/2(3B + G) \tag{4}$$

$$B_V = (C_{11} + C_{22} + C_{33})/9 + 2(C_{12} + C_{13} + C_{23})/9 \tag{5}$$

$$B_R = 1/[(S_{11} + S_{22} + S_{33}) + 2(S_{12} + S_{13} + S_{23})] \tag{6}$$

$$G_V = (C_{11} + C_{22} + C_{33} - C_{12} - C_{13} - C_{23})/15 + (C_{44} + C_{55} + C_{66})/5 \tag{7}$$

$$G_R = 15/[4(S_{11} + S_{22} + S_{33}) - 4(S_{12} + S_{13} + S_{23}) + 3(S_{44} + S_{55} + S_{66})] \tag{8}$$

where G_V and G_R are Voigt shear modulus and Reuss shear modulus, respectively. B_V and B_R are Voigt bulk modulus and Reuss bulk modulus, respectively. S_{ij} is the elastic compliances. The hardness H_v was computed by the Chen model as follows [51],

$$H_v = 2(k^2G)^{0.585} - 3, \tag{9}$$

where the parameter k is the ratio of G/B, and H_v and G are expressed in GPa. Chen model is based on macroscopic parameters and successfully used to estimate the Vickers hardness of TM-B systems [15, 52]. The previously reported methods [53] were adopted for the ideal tensile and shear strength calculations of Hf-B compounds. For the stress–stain relations, a series of incremental tensile/shear stains were applied on a given direction/slip system, until the corresponding conjugate stress components were less than 0 GPa. The minimum tensile or shear ideal strength among all the given directions or slip systems is called the weakest tensile or shear ideal strength.

Results and discussion

Structures and hardness of Hf-B compounds

Hf-B compounds are predicted from the systematic evolutionary searches under ambient and high pressure conditions (Fig. 1). The predicted compounds include $R\bar{3}m$-HfB, $Cmmm$-Hf$_5$B$_6$, $R\bar{3}m$-Hf$_3$B$_4$, Cm-Hf$_3$B$_4$, $Imma$-Hf$_2$B$_3$, $Cmcm$-Hf$_2$B$_3$, Cm-HfB$_3$, $Cmcm$-HfB$_4$, $C2$-HfB$_6$ and $C2/m$-HfB$_8$. Only those in a reasonable range of enthalpies (within 0–0.2 eV/atom from the convex hulls [54]) are plotted among the predicted compounds. Notably, most of the plotted compounds were nearly stable, and their enthalpies were very low. The well-known $P6/mmm$-HfB$_2$ (i.e., h-HfB$_2$) was stable, while the other predicted compounds were metastable (or near stable). The lattice parameters, density, and formation enthalpies of the predicted compounds are listed in Table 1.

The energetic, dynamical and mechanical stabilities confirmed the stability and the synthesis possibility of the predicted Hf-B compounds. From the formation enthalpies shown in Fig. 1 and listed in Table 1, all the considered Hf-B compounds are energetically
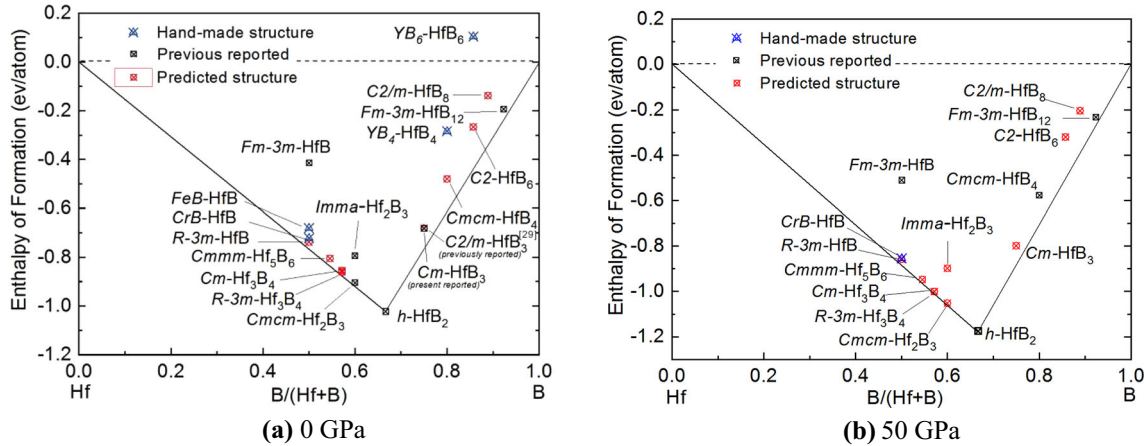
Figure 1 Convex hull of Hf-B system under **a** ambient and **b** high pressure.

stable. The calculated phonon dispersions (see Fig. 2) have no imaginary phonon frequencies throughout the Brillouin zone, suggesting the dynamic stability of Hf-B compounds [55, 56]. The elastic constants C_{ij} (see Table 2), which satisfy criteria of the elastic stability for rhombohedral phase [57], orthorhombic phase [57] and monoclinic phase [58], indicate the mechanical stability of the Hf-B compounds. For the rhombohedral phase, the elastic stability criterion is,

$$C_{11} > |C_{12}|; C_{44} > 0;$$
$$C_{13}^2 < C_{33}(C_{11} + C_{12})/2$$
$$C_{14}^2 + C_{15}^2 < C_{44}(C_{11} - C_{12}) = C_{44}C_{66}$$

(10)

For the orthorhombic phase, the elastic stability criterion is,

$$C_{ii} > 0; C_{ii} + C_{jj} - 2C_{ij} > 0$$
$$C_{11} + C_{22} + C_{33} + 2(C_{12} + C_{13} + C_{13}) > 0$$

(11)

For the monoclinic phase, the elastic stability criterion is,

$$C_{11} > 0; C_{22} > 0; C_{33} > 0; C_{44} > 0; C_{55} > 0; C_{66} > 0; C_{11}$$
$$+ C_{22} + C_{33} + 2C_{12} + 2C_{13} + 2C_{23} > 0; C_{33}C_{55} - C_{35}^2 > 0;$$
$$C_{44}C_{66} - C_{46}^2 > 0; C_{22}C_{33} - 2C_{23}^2 > 0; C_{22}(C_{33}C_{55} - C_{35}^2)$$
$$+ 2C_{23}C_{25}C_{35} - C_{23}^2C_{55} - C_{25}^2C_{33} > 0; \{ 2[C_{15}C_{25}(C_{33}C_{12}$$
$$- C_{13}C_{23}) + C_{15}C_{35}(C_{22}C_{13} - C_{12}C_{23}) + C_{25}C_{35}(C_{11}C_{23}$$
$$- C_{12}C_{13})] - [C_{15}^2(C_{22}C_{33} - C_{23}^2) + C_{25}^2(C_{11}C_{33} - C_{13}^2) + C_{35}^2$$
$$(C_{11}C_{22} - C_{12}^2)] + C_{55}C_{11}C_{22}C_{33} - C_{11}C_{23}^2 - C_{22}C_{13}^2 - C_{33}$$
$$C_{12}^2 + 2C_{12}C_{13}C_{23} \} > 0$$

(12)

Table 1 Lattice parameters (Å), density (g/cm³), formation enthalpy (eV/atom) of hafnium borides at ambient pressure

| Structure type	Species	Lattice parameters			Density	Formation enthalpy
		a	b	c		
Sandwiches I	$R\bar{3}m$-HfB	3.156	12.459	3.156	11.812	−0.738
	$R\bar{3}m$-Hf₃B₄	3.151	5.458	9.8	11.601	−0.861
	$Imma$-Hf₂B₃	3.145	7.58	5.493	10.879	−0.793
	$P6/mmm$-HfB₂	3.143	/	3.485	11.140	−1.022
	Cm-HfB₃	5.407	5.434	9.104	9.542	−0.680
	$Cmcm$-HfB₄	5.361	3.135	10.356	8.458	−0.480
	$C2$-HfB₆	5.321	3.155	7.406	7.153	−0.267
	$C2/m$-HfB₈	8.286	5.451	3.095	6.314	−0.138
Sandwiches II	CrB-HfB	3.514	9.164	3.228	12.096	−0.722
	$Cmmm$-Hf₅B₆	3.199	3.505	12.031	11.929	−0.805
	Cm-Hf₃B₄	6.368	7.694	3.502	11.77	−0.855
	$Cmcm$-Hf₂B₃	9.693	3.013	3.287	11.626	−0.904
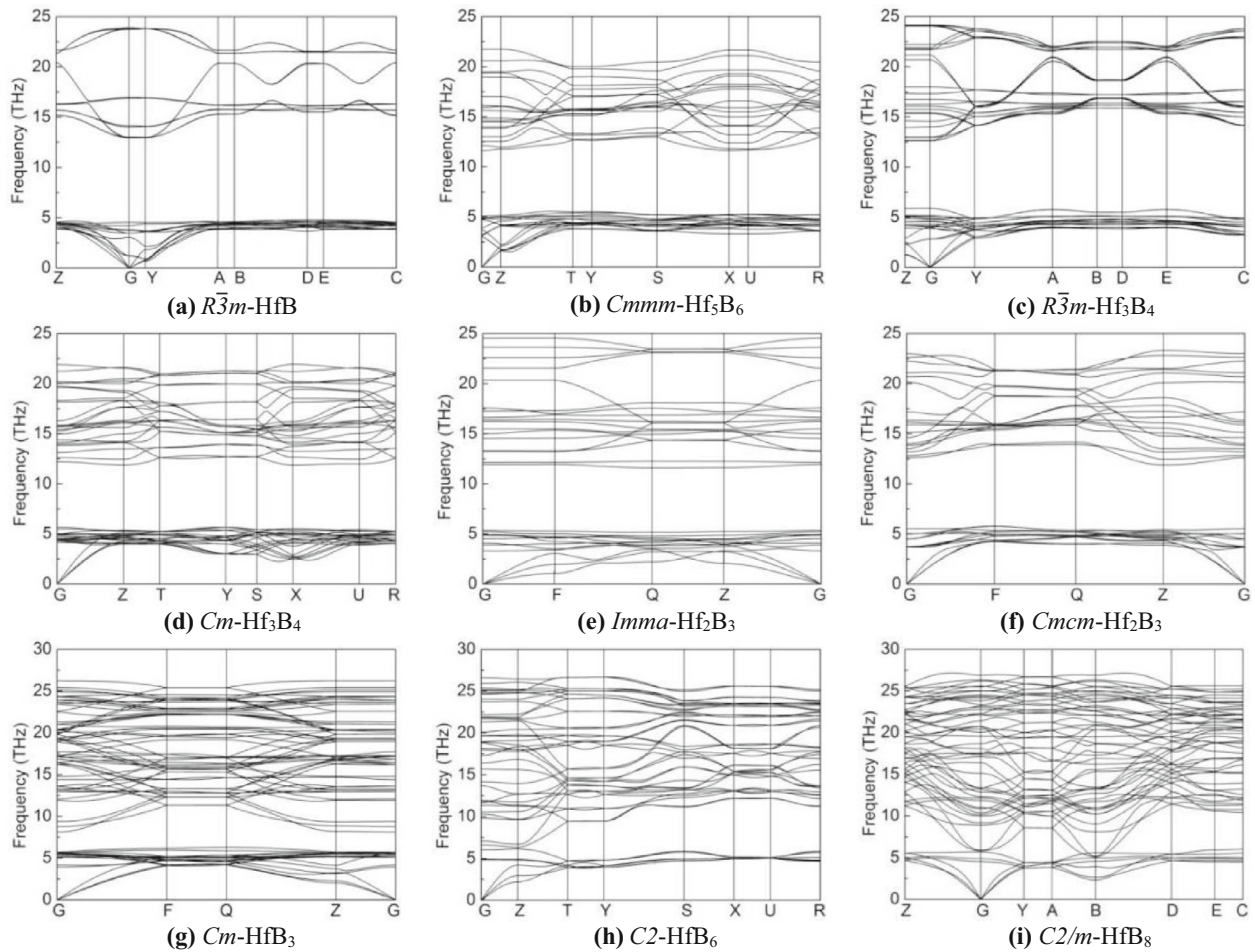
Figure 2 Phonon spectra of the predicted Hf-B phases at ambient pressure.

Table 2 Elastic constants of newly predicted Hf-B phases at ambient pressure

Structure type	Species	C11	C22	C33	C44	C55	C66	C12	C13	C23	C15	C25	C35	C46
Sandwiches I	$R\bar{3}m$-HfB	419.7	322	429.6	71	65.8	176.7	77.6	59.2	72.1				
	$R\bar{3}m$-Hf$_3$B$_4$	490	492.3	360.7	209.6	109.9	113.5	55.3	98.5	94				
	$Imma$-Hf$_2$B$_3$	522.6	324.8	369.5	167.3	90.7	188.4	71.4	62.3	130.2				
	Cm-HfB$_3$	585.7	593.1	509	265.6	184.8	216.9	62.2	108.5	109.5	−8.4	9.7	31.5	0.9
	$C2$-HfB$_6$	631.3	626.5	543.9	262.6	265.9	227	56.6	82.2	80	−0.7	−0.02	4.1	2.9
	$C2/m$-HfB$_8$	563.5	579.8	605.8	241	265.8	211.7	82	79.3	85.7	−0.6	12.6	−28	20.4
Sandwiches II	$Cmmm$-Hf$_5$B$_6$	480.7	437	430.9	192.7	158.9	194.3	85.5	83.5	86.6				
	Cm-Hf$_3$B$_4$	512	428.9	408.9	211.2	205	207.6	76.9	92.2	129.4	1.3	12.3	−13.8	−0.2
	$Cmcm$-Hf$_2$B$_3$	494.5	531.9	468.9	220.4	213.5	188.4	77	93.5	94.1				

Note that metastable structures can often be synthesized by choosing appropriate conditions [59]. For example, the newly predicted $R\bar{3}m$-HfB and handmade FeB-HfB compounds have more than 0.2 eV/atom lower enthalpy than the previously reported experimentally synthesized $Fm\bar{3}m$-HfB. It suggests

higher energetic stability and synthesis possibility of $R\bar{3}m$-HfB and FeB-HfB compounds than $Fm\bar{3}m$-HfB.

Notably, the predicted Hf-B compounds with high B concentration (B/(Hf + B) > 0.66) are all estimated to be superhard (> 40 GPa). The relevant values related to hardness are 45.4 GPa for $P6/mmm$-HfB$_2$,

40.2 GPa for Cm-HfB$_3$, 45.6 GPa for $Cmcm$-HfB$_4$, 50 GPa for $C2$-HfB$_6$, and 45.1 GPa for $C2/m$-HfB$_8$ (see Fig. 3). The predicted $C2$-HfB$_6$ has the highest hardness than all the other previously reported Hf-B compounds [28, 33].

For the predicted Hf-B compounds with B/(Hf + B) < 0.66, the hardness is less than 40 GPa. These compounds include $R\overline{3}m$-HfB (16.3 GPa), $R\overline{3}m$-Hf$_3$B$_4$ (23.9 GPa), $Imma$-Hf$_2$B$_3$ (23.3 GPa), CrB-HfB (29.1 GPa), $Cmmm$-Hf$_5$B$_6$ (33 GPa), Cm-Hf$_3$B$_4$ (35 GPa) and $Cmcm$-Hf$_2$B$_3$ (37.7 GPa). Some of these Hf-B compounds have the same B/(Hf + B) ratio, i.e., $Imma$-Hf$_2$B$_3$ and $Cmcm$-Hf$_2$B$_3$, but different structures and hardness.

The structures of predicted Hf-B compounds can be divided into two types, as shown in Fig. 4. The first type is referred to as sandwich I structure, which is an AlB$_2$-type sandwich-like structure with interval 2-D or 3-D Hf layer or B layer. The second type is referred to as sandwich II structure, which is a sandwich-like structure with mixing Hf and B atoms in the same planar layer.

The $P6/mmm$-HfB$_2$ (Fig. 4g) has the typical sandwiches I structure. The coplanar graphite-like B layers are present alternatively with the close-packed Hf sheets, which can be regarded as B-Hf sandwiches stacking along the axis. Similarly, $R\overline{3}m$-HfB and $R\overline{3}m$-Hf$_3$B$_4$ can be described as hafnium-rich (compared to HfB$_2$) Hf-B-Hf and Hf-B-Hf-B-Hf sandwiches, respectively. The Cm-HfB$_3$, $C2$-HfB$_6$ and $C2/m$-HfB$_8$ can be described as boron-rich (compared to HfB$_2$) B-Hf-B-B-Hf-B, B-B-B-Hf and B-B-B-B-Hf

sandwiches, respectively. B remains in the form of B–B bonding membered rings for sandwiches II structure, while the Hf atom from the neighboring layer is located in the center of the B–B rings. The predicted $Cmmm$-Hf$_5$B$_6$, Cm-Hf$_3$B$_4$ and $Cmcm$-Hf$_2$B$_3$ and handmade CrB-HfB all have the sandwiches II structure and B/(Hf + B) ratio lower than 0.67.

According to the structures and B concentrations, Hf-B compounds of sandwiches I structure with B/(Hf + B) ≥ 0.66 and B/(Hf + B) < 0.66 can be classified as Group A and Group B, respectively. Hf-B compounds with sandwiches II structure is regarded as Group C. As shown in Fig. 3, Hf-B compounds of Group A possess superhardness (> 40 GPa). The Hf-B compounds (B/(Hf + B) < 0.66) of Group B have a sandwiches I structure but has lower hardness as compared to Group A. The hardness of Hf-B compounds of Group C is lower than 40 GPa, but increases from 29.1 GPa (CrB-HfB) to 37.7 GPa ($Cmcm$-Hf$_2$B$_3$) with the increase of B/(Hf + B) ratio.

Both boron concentration and compounds structure greatly influence the hardness of the studied Hf-B compounds. The reason behind the difference in hardness of the Hf-B compounds will be explained from their elastic properties and chemical bonding in the following section.

Elastic properties and chemical bonding

The bulk modulus B, shear modulus G, Young's modulus Y and Poisson's ratio v were extracted from the elastic constants to explain of the variety of the hardness of Hf-B compounds. It is proposed that shear modulus G is more accurate than bulk modulus B in evaluating the potential hardness of polycrystalline materials [60]. Young's modulus Y is also a vital parameter to value the stiffness of a material. The calculated results are presented in Table 3 and Fig. 5. For comparison, values of the reported compounds $Fm\overline{3}m$-HfB, $P6/mmm$-HfB$_2$, $Cmcm$-HfB$_4$ and $Fm\overline{3}m$-HfB$_{12}$ are listed in Table 3. Our calculated data have good agreement with the previously reported data, confirming the reliability of the calculations in this study.

For the Hf-B compounds of Group A (sandwiches I structure, B/(Hf + B) > 0.66), both of the bulk modulus B and shear modulus G are higher than 220 GPa, indicating good ability of Group A compounds against the volume deformation and the shear strain. The Young's modulus Y of Group A compounds is in
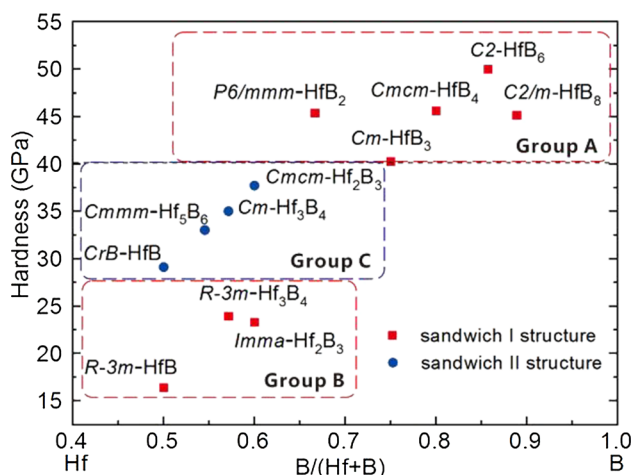

Figure 3 The calculated hardness of Hf-B compounds with sandwiches I and II structures.
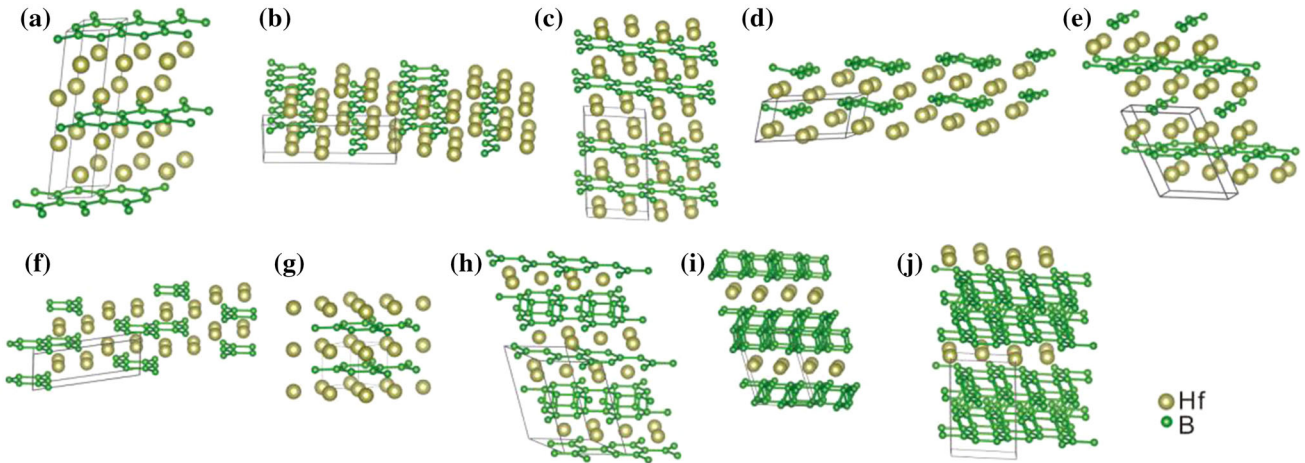
Figure 4 Structures of predicted Hf-B **a** $R\bar{3}m$-HfB, **b** $Cmmm$ -Hf$_5$B$_6$, **c** $R\bar{3}m$-Hf$_3$B$_4$ **d** Cm-Hf$_3$B$_4$, **e** $Imma$-Hf$_2$B$_3$, **f** $Cmcm$ -Hf$_2$B$_3$, **g** the well-known AlB$_2$-type $P6/mmm$-HfB$_2$ (i.e., h-HfB$_2$), **h** Cm -HfB$_3$, **i** $C2$-HfB$_6$, and **j** $C2/m$-HfB$_8$. (The structure type of $R3m$-HfB, $R3m$-Hf$_3$B$_4$, $Imma$-Hf$_2$B$_3$, $P6/mmm$-HfB$_2$, Cm-HfB$_3$, $C2$-HfB$_6$, and $C2/m$-HfB$_8$ is referred as sandwiches I structure. The structure type of $Cmmm$-Hf$_5$B$_6$, Cm-Hf$_3$B$_4$ and $Cmcm$-Hf$_2$B$_3$ is referred as sandwiches II structure.).

Table 3 Bulk modulus B (GPa), shear modulus G (GPa), Young's modulus Y (GPa), B/G ratio, Poisson's ratio (v) and Debye temperature Θ (K) and hardness H_v (GPa) of hafnium borides at ambient pressure

Structure type	Group	Species	B	G	Y	B/G	v	Θ	H_v
Sandwiches I	B	$R\bar{3}m$-HfB	176	114	282	1.53	0.233	433	16.4
		$R\bar{3}m$-Hf$_3$B$_4$	203	152	365	1.34	0.200	522	23.9
		$Imma$-Hf$_2$B$_3$	193	145	347	1.33	0.199	526	23.3
	A	$P6/mmm$-HfB$_2$	253	246	558	1.03	0.133	714	45.4
		$P6/mmm$-HfB$_2$ [a]	263	249					
		Cm-HfB$_3$	241	223	511	1.08	0.146	755	40.3
		$C2/m$-HfB$_3$ [b]	248	229	525	1.09	0.147		40.8
		$Cmcm$-HfB$_4$	245	241	544	1.02	0.130	847	45.6
		$Cmcm$-HfB$_4$ [c]	243	240	542	0.987	0.128	845	45.7
		$C2$-HfB$_6$	249	256	571	0.97	0.117	972	50
		$C2/m$-HfB$_8$	249	243	549	1.03	0.133	1023	45.1
Sandwiches II	C	CrB-HfB	194	163	382	1.19	0.172	512	29.1
		CrB-HfB [d]	207.7	171.9	408.2	1.19	0.172		26.3
		$Cmmm$-Hf$_5$B$_6$	206	181	421	1.14	0.160	556	33
		Cm-Hf$_3$B$_4$	216	193	446	1.12	0.156	584	35
		$Cmcm$-Hf$_2$B$_3$	224	206	473	1.09	0.149	616	37.7

[a]Reference [61]

[b]Reference[32]

[c]Reference[33]

[d]Reference[13]

the range of 511–571 GPa (as listed in the Table 3). Hf-B compounds of Group B and C have much lower value of bulk modulus B, shear modulus G and Young's modulus Y than that of Group A. For the Group C compounds with sandwiches II structure, the value of B, G and Y give the increasing trend from 194 to 224 GPa, 163 to 206 GPa, and 382 to 473 GPa, respectively, with the increase of B/(Hf + B) ratio. Although Group B and C Hf-B compounds have the same B/(Hf + B) ratio (such as CrB-HfB and $R\bar{3}m$-HfB, Cm-Hf$_3$B$_4$ and $R\bar{3}m$-Hf$_3$B$_4$, $Cmcm$-Hf$_2$B$_3$ and $Imma$-Hf$_2$B$_3$), Group B compounds have higher value of bulk modulus B, shear modulus G and Young's modulus Y than that of the Group C compounds.
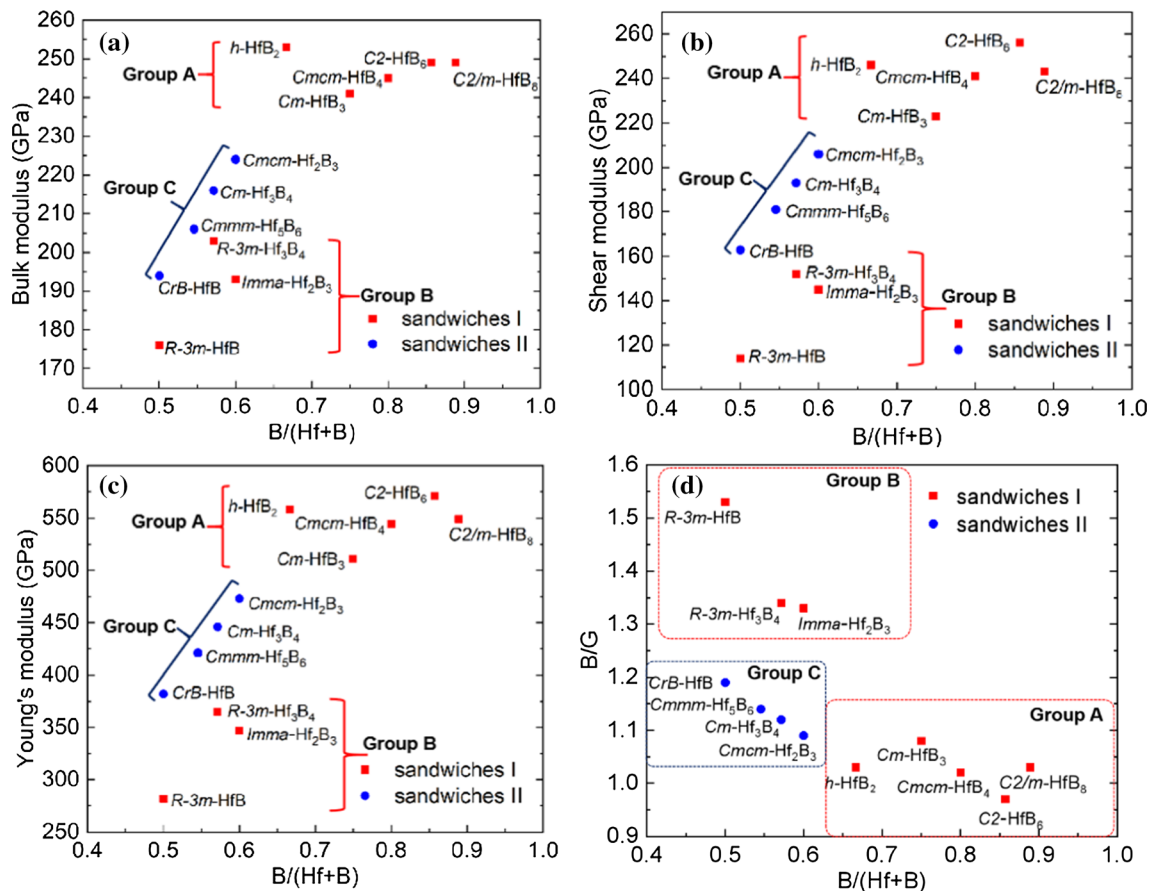
Figure 5 The calculated **a** bulk modulus B, **b** shear modulus G, **c** Young's modulus Y and **d** B/G of Hf-B compounds with sandwiches I and II structures.

This is because of their different sandwiches structures and chemical bonding, which will be described later in this section.

Due to the high bulk modulus B, shear modulus G and Young's modulus Y, it is reasonable to conclude that the Hf-B compounds of Group A possess high hardness. It is consistent with the calculated hardness presented in Fig. 3. The changing trends of the calculated hardness of Group B and C compounds, as listed in Table 3 and shown in Fig. 3 and 5a–c, are also consistent with corresponding B, G and Y values. Among all the considered Hf-B compounds, $C2$-HfB$_6$, which possesses an estimated hardness of up to 50 GPa, has the highest shear modulus G and the highest Young's modulus Y.

The Pugh ratio [62] B/G is frequently used to describe the ductility of a material. For ductile materials, the B/G is > 1.75, and for brittle materials, the B/G is < 1.75. As the value listed in Table 3, all the considered Hf-B compounds (Group A, B and C) have a B/G ratio smaller than 1.75, implying their

brittle nature [62] (for Al, B/G = 2.74, for diamond, B/G = 0.8, for c-BN B/G = 0.96). As shown in Fig. 5d, the B/G of Group A Hf-B compounds (B/(Hf + B) > 0.66) is higher than that of the Group B compounds (B/(Hf + B) < 0.66). For Group C Hf-B compounds, the B/G have a linear relationship with boron concentration. Higher Debye temperature Θ reflects to a higher melting temperature and stronger atomic bonding. The value of Debye temperature Θ of the Hf-B compounds from the same group increases with the B/(Hf + B) ratio. For example, the Debye temperature Θ of Hf-B compounds in Group A increases from 714 K for h-HfB$_2$ to 1023 K for $C2/m$-HfB$_8$. Moreover, the Debye temperature Θ of Group A is higher than Group B and C. The Hf-B compounds from Group B have higher Θ value than those from Group C with the same B/(Hf + B) ratio. Poisson's ratio v is a key parameter to indicate the directionality for chemical bonding. Covalent materials and metallic materials have a typical v value of 0.1 and 0.33, respectively. The values of v for all the

Hf-B compounds of Group A, B and C are lower than 0.2, except for $R\bar{3}m$-HfB of Group B. It indicates their strong covalent bond characteristics. Among them, the v of 0.117 for $C2$-HfB$_6$ is closest to 0.1.

In order to further explain the variation in the elastic properties of different Hf-B compounds, the total density of states (TDOS) and partial density of states (PDOS), which reflect the chemical bonding, were calculated, as given in Fig. 6.

All the hafnium borides are weak metal due to the finite but small DOS values at Fermi level E_f. For the Group B and C Hf-B compounds with B/(Hf + B) < 0.66, the TDOS near the Fermi level E_f is contributed mainly by the Hf-5p and Hf-5d states with a small contribution from B-2p. Therefore, metallic properties of Group B and C compounds are mainly due to the Hf-5p and Hf-5d electrons. For the Group A Hf-B compounds with B/(Hf + B) > 0.66 the Fermi level E_f is mainly derived from Hf-5d and B-2p electrons, indicating the highly mixed metallic covalent. Moreover, B-2p electrons have significant contribution under the energy higher than − 8 V, and the strong covalent lead to superhardness of the group A Hf-B compounds.

In the PDOS of Group B and C Hf-B compounds, Hf-5d, Hf-5p and B-2p orbitals have similar profiles from − 6 to 0 V, indicating their hybridization and significant covalent interaction between Hf and B. Especially for $Cmmm$-Hf$_5$B$_6$, Cm-Hf$_3$B$_4$ and $Cmcm$-Hf$_2$B$_3$ from Group C (Fig. 6c, g, k), the profiles of Hf-5d, Hf-5p and B-2p orbitals, from − 4 to 0 V, are nearly the identical. It is because of the mixing of Hf and B atoms in the intra and interlayer of sandwiches II structure. Compared to Group B Hf-B compounds with the sandwiches I structure, Group C Hf-B compounds with the same B/(Hf + B) ratio but with a sandwiches II structure have stronger hybridization, contributing to higher hardness. Examples of such compounds are $Imma$-Hf$_2$B$_3$ from Group B and $Cmcm$-Hf$_2$B3$_3$ from Group C.

Ideal strength

Weakest ideal strength

To further confirm the intrinsic hardness of the predicted compounds, the ideal strength of the Hf-B compounds were calculated by continuously applying tensile and shear strains until the bonds were broken. Note that the above elastic properties and hardness were calculated based on the limited value of the strain–stress relation.

Under tensile loads (see Fig. 7), the weakest ideal tensile strengths of Cm-HfB$_3$, $Cmcm$-HfB$_4$, $C2$-HfB$_6$ and $C2/m$-HfB$_8$, with the sandwiches I structure, are calculated as 8.1 GPa in [011] direction, 18.7 GPa in [011] direction, 27.6 GPa in [010] direction, and 23.8 GPa in [011] direction, respectively. For sandwiches II structure, $Cmmm$-Hf$_5$B$_6$, Cm-Hf$_3$B$_4$ and $Cmcm$-Hf$_2$B$_3$ have the weakest ideal tensile strengths with values 13.9, 17.3 and 18.8 GPa, respectively, in [010] direction.

In the case of shear loads, various slip systems were systematically studied under shear deformations (see Fig. 8). The weakest shear strengths of $Cmmm$-Hf$_5$B$_6$, Cm-Hf$_3$B$_4$ and $Cmcm$-Hf$_2$B$_3$ are found to be 28.3 GPa in (010)< 010 > system, 31.6 GPa in (100)< 010 > system, and 28.9 GPa in (100)< 010 > system, respectively. However, the weakest shear strengths of the Cm-HfB$_3$, $Cmcm$-HfB$_4$, $C2$-HfB$_6$ and $C2/m$-HfB$_8$ are as low as 3.4 GPa in (010)< 001 > system, 8.3 GPa in (001)< 110 > system, 14.9 GPa in (001)< 110 > system, and 10.3 GPa in (010)< 101 > system, respectively. However, the maximum peak tensile and shear strengths of the calculated Hf-B compounds are all above 40 GPa. It indicates their strong anisotropy.

Accordingly, the weakest ideal strengths Hf-B compounds with sandwiches I structure (i.e., Cm-HfB$_3$, $Cmcm$-HfB$_4$, $C2$-HfB$_6$ and $C2/m$-HfB$_8$) and with sandwiches II structure (i.e., $Cmmm$-Hf$_5$B$_6$, Cm-Hf$_3$B$_4$ and $Cmcm$-Hf$_2$B$_3$) are plotted in Fig. 9. Note that the weakest ideal strength values of all these Hf-B compounds are lower than that of h-HfB$_2$, which is 33.3 GPa along (10–10)<− 12–10> system [63].

Bond-breaking mechanism

The bond-breaking mechanism in the weakest pure deformation direction is further explored to explain the low ideal strengths of the predicted Hf-B phases.

For the Hf-B compounds (B/(Hf + B) > 0.66) with the sandwiches I structure, after applying shear load, the increasing bond-lengths of the "key" Hf-B bonds lead to the big jump in the angle of the three-dimensional (3-D) boron network (i.e., changing the shape of the network). This change in the shape of the boron network leads to the rearrangement of the sp^2 hybridization of B–B bonds, and the structural collapse (see Figs. 10, 11, 12, 13). Taking $C2$-HfB$_6$ for
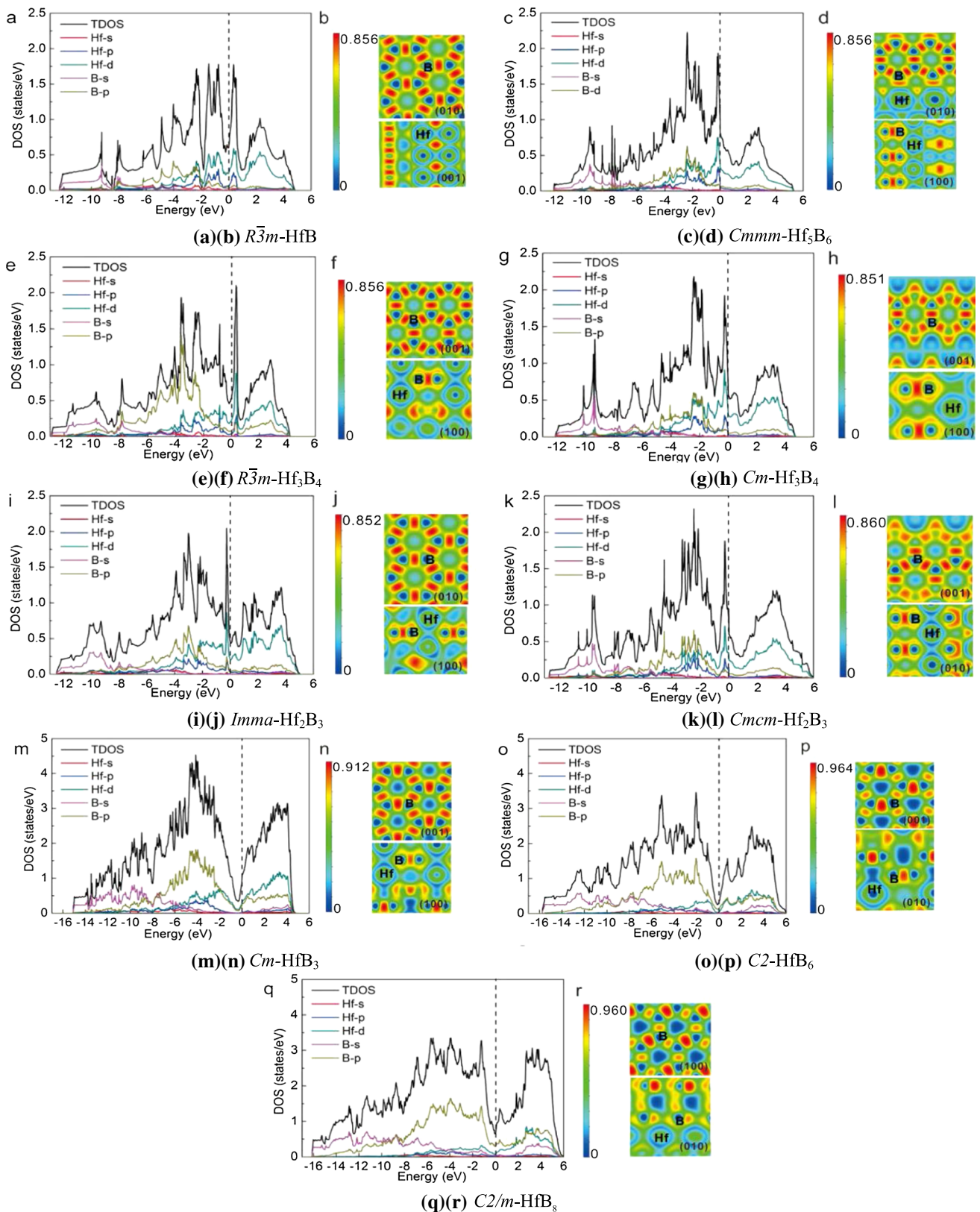
Figure 6 Density of states and electronic localization function (ELF) of the predicted Hf-B compounds.
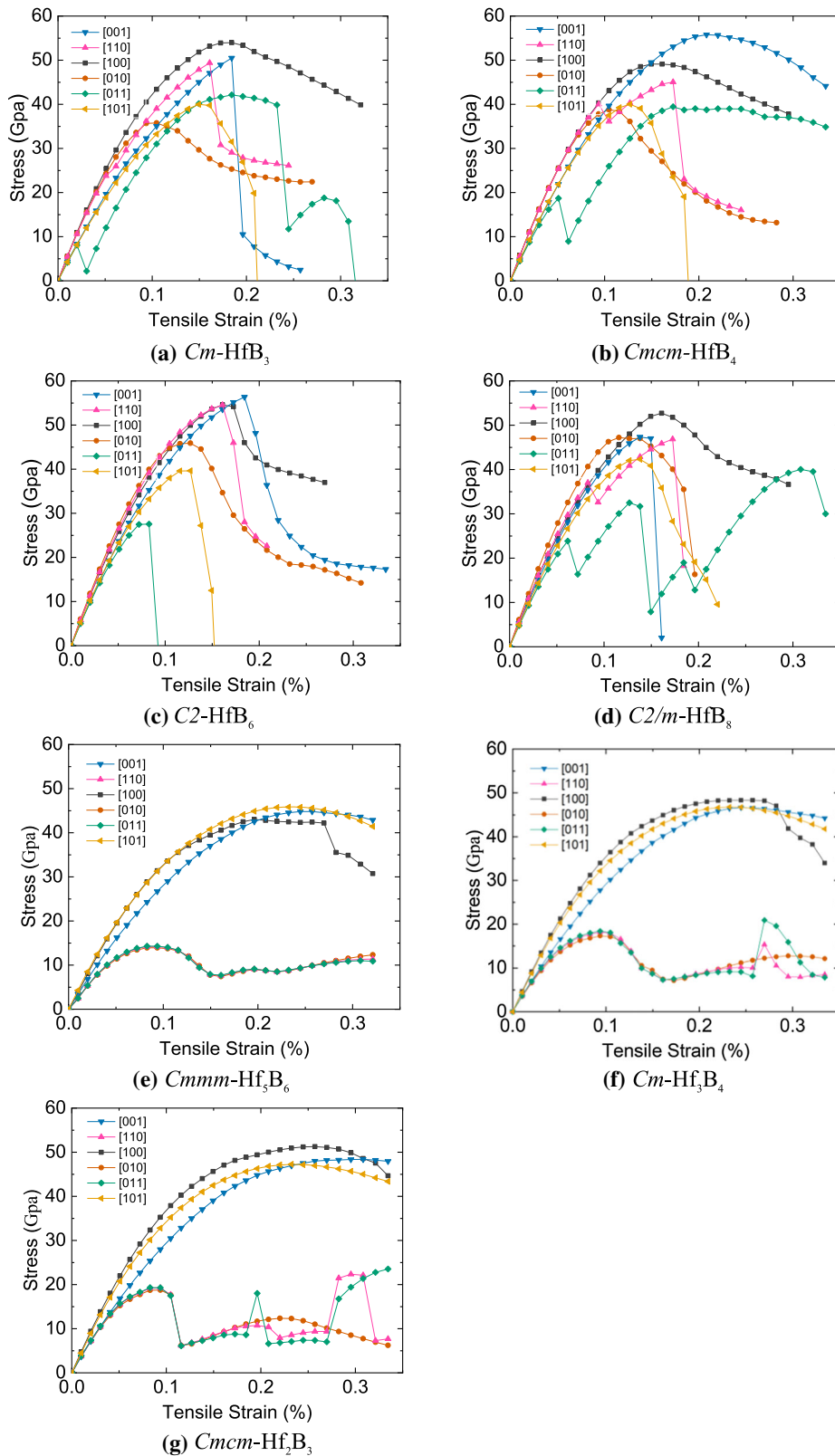
Figure 7 The calculated stress–strain relations of Hf-B with sandwiches I and II structures under various tensile loads.
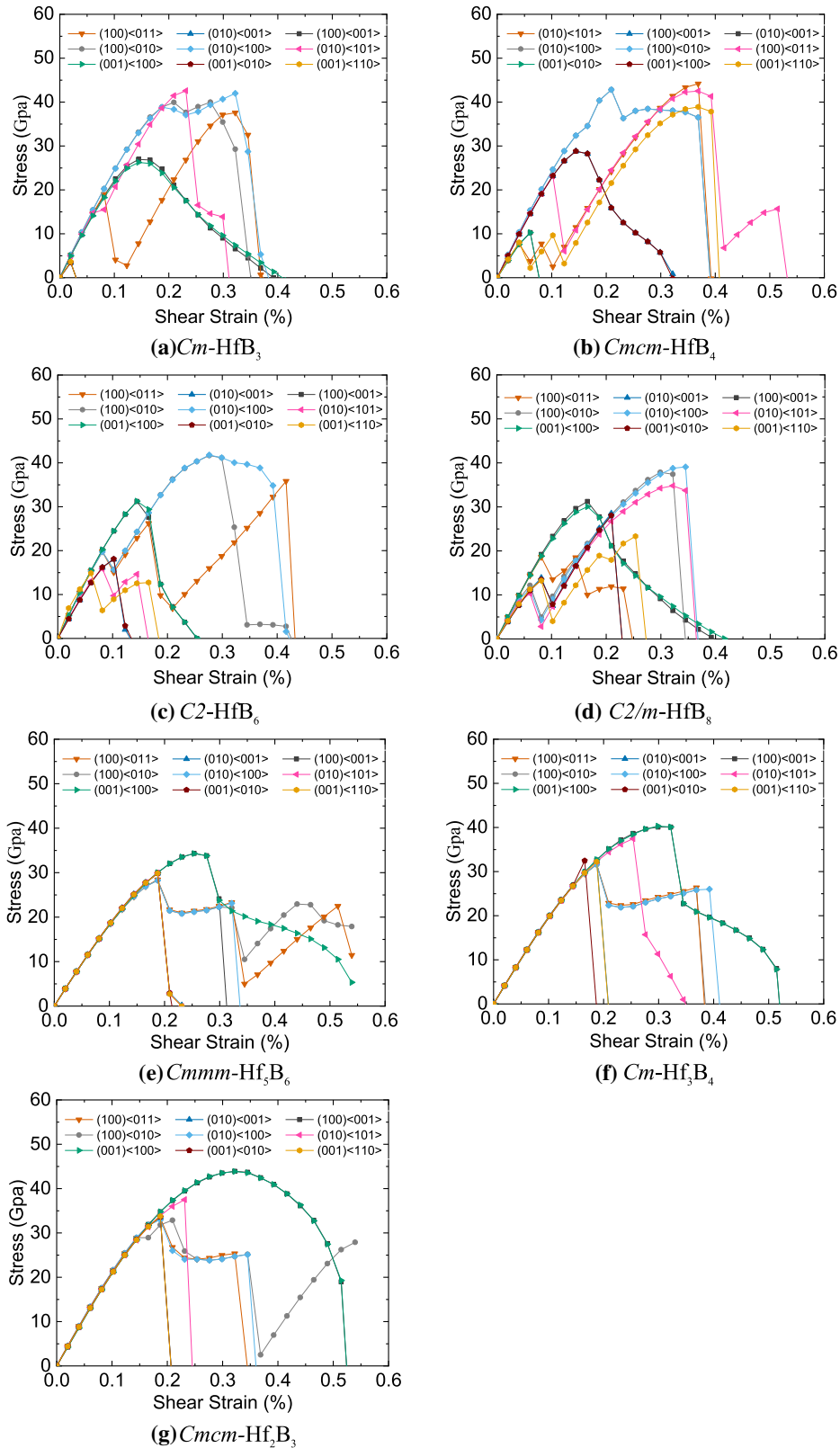
Figure 8 The calculated stress–strain relations of Hf-B with sandwiches I and II structures under various shear loads.

example (Fig. 12), the bond-lengths dramatically change from 2.450 (at $\varepsilon = 0.0606$) to 2.541 Å (at $\varepsilon = 0.0812$) for Hf_2-B_2 bond, and from 2.630 (at $\varepsilon = 0.0606$) to 2.518 Å (at $\varepsilon = 0.0812$) for Hf_2-B_6 bond. Nevertheless, B–B bond-lengths of C_2-HfB_6 have no apparent changes and the angles of B atoms show a big jump, indicating the significant changes of the shape of the boron network. Instead of the broken of

Figure 9 The weakest ideal strengths of Hf-B compounds with two different types of sandwiches structures ([e]Reference [64], [f]Reference [34]).

B–B bonds (such as FeB_4 [65]), the "deformity" of 3-D boron network and the corresponding charge transfer cause the structural collapse of the calculated Hf-B compounds with the sandwiches I structure under specific loading deformation.

For the tensile deformation, the increasing of bond-length of Hf_1-B_9 is the most critical factor in determining the tensile strength of $Cmcm$-Hf_2B_3 in [010] direction (see Fig. 14e, f), even though the bonding between B1–B5 atoms becomes more robust due to shorter bond-length. A similar phenomenon can also be observed in the case of $Cmmm$-Hf_5B_6 and Cm-Hf_3B_4 with sandwiches II structures when applying tensile deformation (Fig. 14a–d).

According to the calculation results in this paper, the mechanical properties of the Hf-B compounds with sandwiches II structure (Group C) have a linear relationship with the B content. Bulk modulus B, shear modulus G, Young's modulus Y, hardness H_v and the weakest ideal strength of Group C compounds all increase with B concentration. Because of the highest amount of boron content among all the considered Group C compounds, $Cmcm$-Hf_2B_3 has the highest values in B, G, Y, H_v and weakest ideal strength due to stronger B covalent bond and hybridization interaction between Hf and B atoms. Moreover, the structural failure of Group C compounds under tensile deformation is caused by the
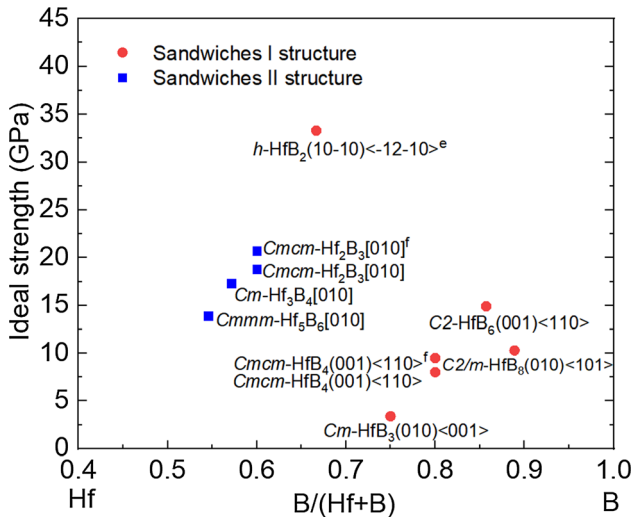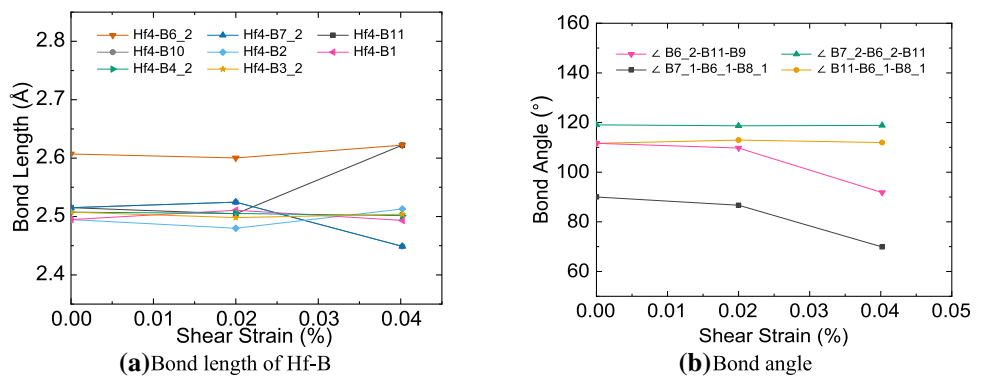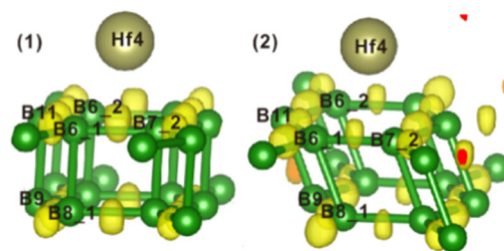
Figure 10 The variations of bond lengths, bond angles and ELF of Cm-HfB_3 under shear load in (010)< 001 > slip system (see variations of bond length B–B in Fig. S1 of supplementary material).

(a) Bond length of Hf-B

(b) Bond angle

(c) ELF of the deformation structure under shear strain of (1) $\varepsilon = 0$ and (2) $\varepsilon = 0.04$

Figure 11 The variations of bond lengths, bond angles and ELF of *Cmcm*-HfB$_4$ under shear load in (010)< 001 > slip system (see variations of bond length B–B in Fig. S2 of supplementary material).
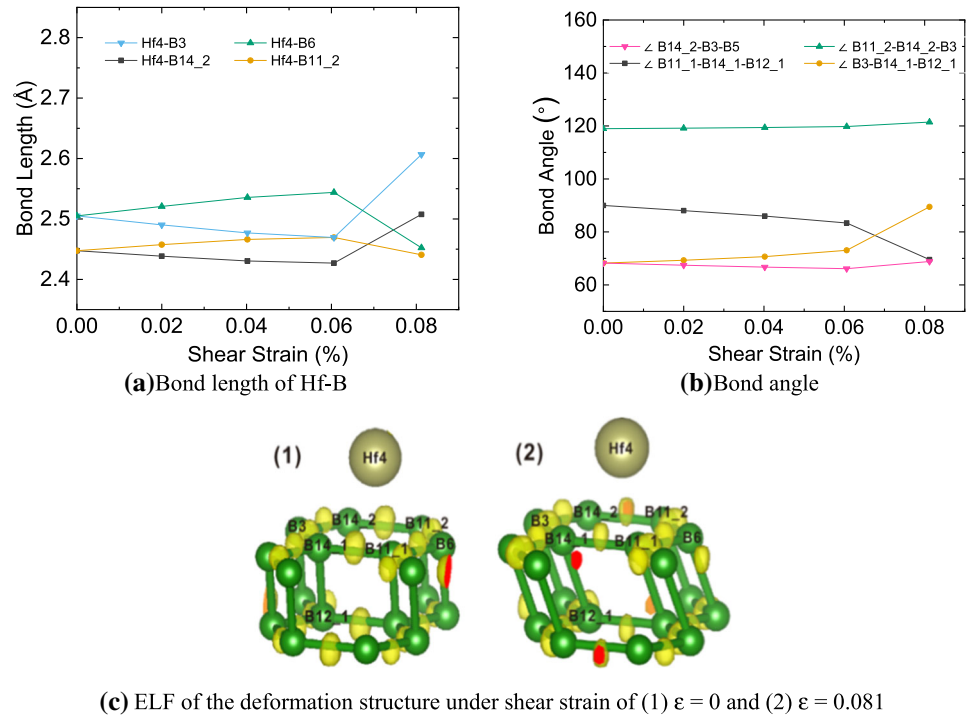

(a) Bond length of Hf-B

(b) Bond angle

(c) ELF of the deformation structure under shear strain of (1) ε = 0 and (2) ε = 0.081

Figure 12 The variations of bond lengths, bond angles and ELF of *C2*-HfB$_6$ under shear load in (001)< 110 > slip system (see ELF and related atom number in Fig. S3 of supplementary material).
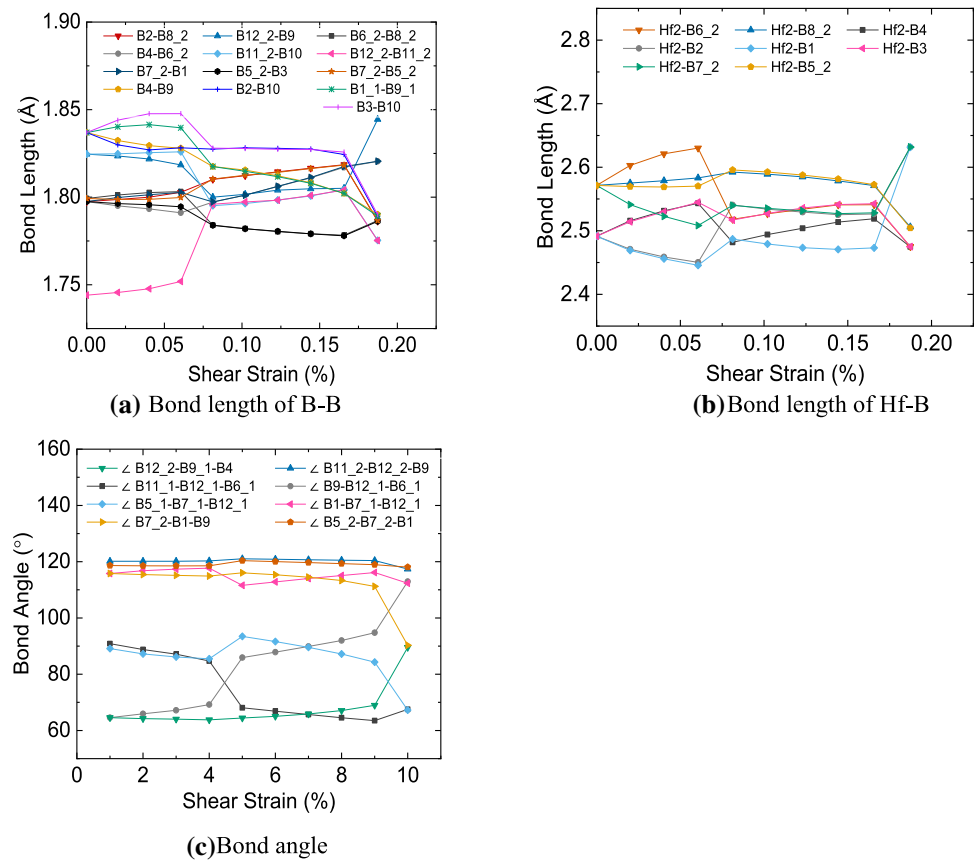

(a) Bond length of B-B

(b) Bond length of Hf-B

(c) Bond angle

Figure 13 The variations of bond lengths, bond angles and ELF of $C2/m$-HfB$_8$ under shear load in $(100)<011>$ slip system (see ELF and related atom number in Fig. S4 of supplementary material).
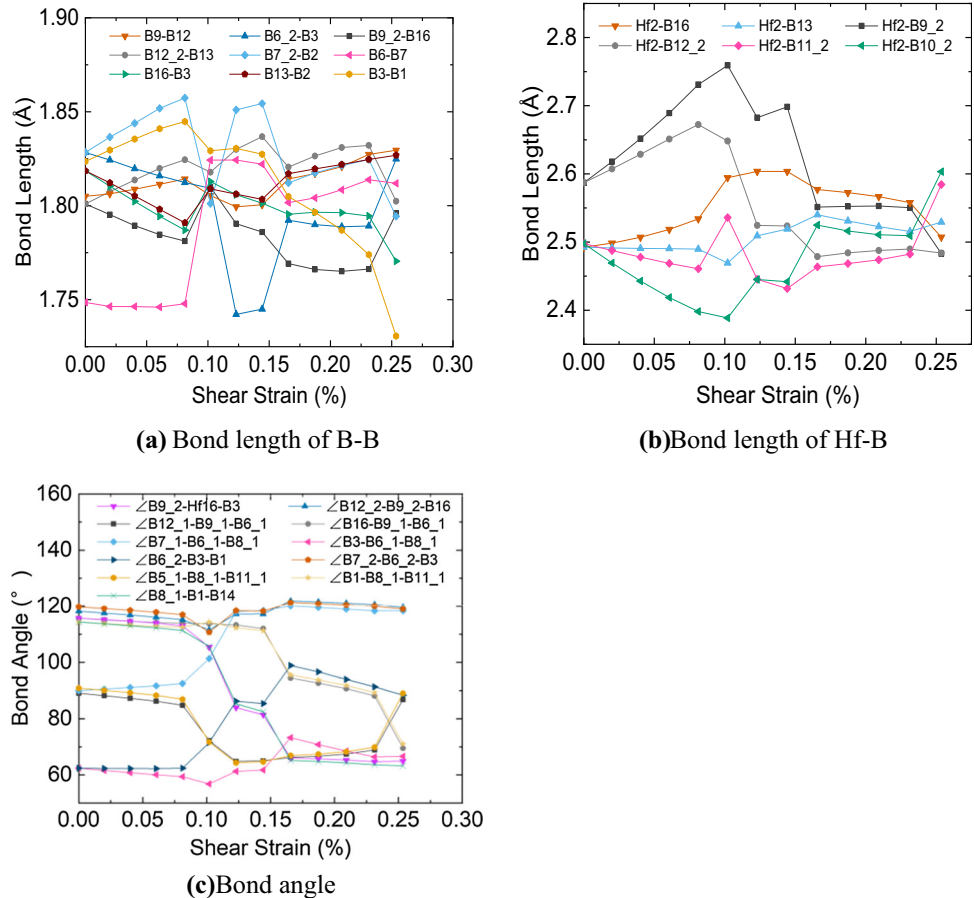

(a) Bond length of B-B

(b) Bond length of Hf-B

(c) Bond angle

broken of Hf-B bond. Therefore, stronger hybridization interaction of Hf and B atoms can increase the ideal strength of Group C Hf-B compounds with sandwiches II structure.

For Hf-B phases with sandwiches I structure (Group A and B), there is no apparent linear relationship between B concentration and the change trend of mechanical properties. According to the analysis of chemical bonding in Elastic properties and chemical bonding Section, higher B concentration leads to stronger B covalent bonds in Hf-B compounds. It leads to higher elastic properties such as B, G, Y and H_v, especially for Group A Hf-B compounds with $B/(Hf + B) > 0.66$. However, due to the relatively weak hybridization interaction between Hf and B bonds of Group A Hf-B compounds, the 3-D boron network is deformed during the shearing deformation under applying relative small shear load, leading to the structure deformation failure but with small change of B–B bond lengths. Therefore, Hf-B compounds with high $B/(Hf + B)$
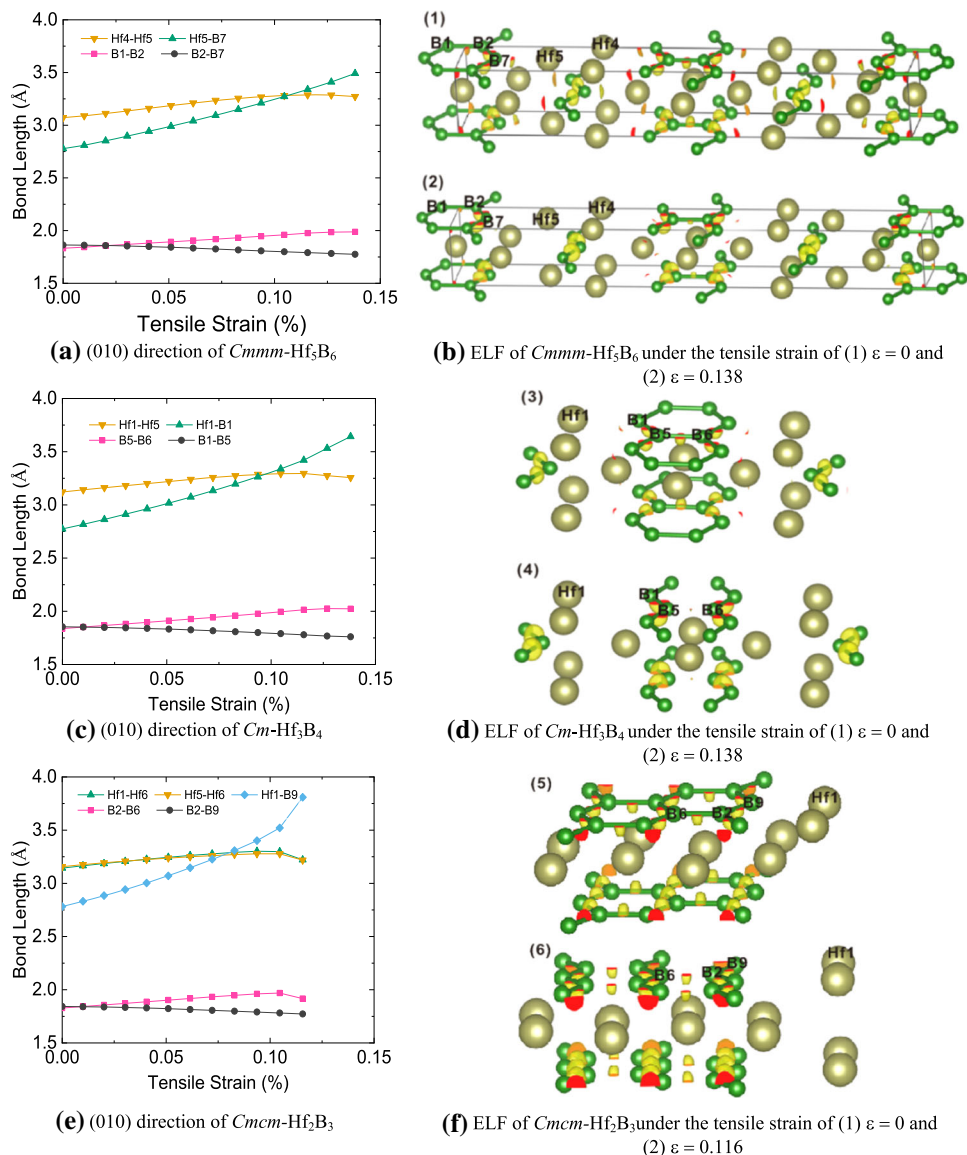
ratio and strong covalent bond are not "doomed" to be material with high value of "weakest ideal strength". A similar phenomenon was also found in the case of B-C-O system [64].

Among all the calculated Hf-B structures, considering the structural stability and mechanical properties, we consider that the $P6/mmm$-HfB$_2$ and $Cmcm$-Hf$_2$B$_3$ structures have high potential for engineering applications. The results in this study may also provide an idea for the design of TM-B structures with high mechanical properties, i.e., through improving the hybridization of TM-B atoms while maintaining a high B concentration.

Conclusions

This study explored the previously unknown structures of the Hf-B compounds. Moreover, the correlation of the Hf-B compound structures with mechanical properties was investigated through theoretical calculation.

Figure 14 The variations of bond lengths and ELF of Hf-B with sandwiches II structure under tensile loads.

(a) (010) direction of *Cmmm*-Hf₅B₆

(b) ELF of *Cmmm*-Hf₅B₆ under the tensile strain of (1) ε = 0 and (2) ε = 0.138

(c) (010) direction of *Cm*-Hf₃B₄

(d) ELF of *Cm*-Hf₃B₄ under the tensile strain of (1) ε = 0 and (2) ε = 0.138

(e) (010) direction of *Cmcm*-Hf₂B₃

(f) ELF of *Cmcm*-Hf₂B₃under the tensile strain of (1) ε = 0 and (2) ε = 0.116

Potential crystal structures of Hf-B compounds, which have energetic stability, dynamic stability and mechanical stability, are predicted from the systematic evolutionary searches. According to the B concentration and sandwiches structure types, the studied Hf-B compounds were classified as Group A (sandwiches I structure and high B concentration B/(Hf + B) > 0.66), Group B (sandwiches I structure and low B concentration B/(Hf + B) < 0.66) and Group C (sandwiches II structure and low B concentration B/(Hf + B) < 0.66).

Originated from the strong covalent bonding between B–B atoms, *Cm*-HfB₃, *Cmcm*-HfB₄, *C2*-HfB₆, and *C2/m*-HfB₈ from Group A Hf-B compounds have superhardness. Significantly, the newly predicted *C2*-

HfB₆ had hardness up to 50 GPa, which is the highest among all the previously reported Hf-B compounds. Group A Hf-B compounds have obviously lower value of bulk modulus B, shear modulus G, Young's modulus Y, and hardness H_v than that of Group B and C compounds. The estimated B, G, Y, H_v and the weakest ideal strengths of Group C compounds had positive linear relationship with B concentrations. This is because of stronger hybridization interaction between Hf and B atoms for Group C compounds when their B concentrations are higher. Low values (< 20 GPa) of the weakest ideal tensile/shear strengths were obtained for Hf-B compounds with different sandwiches structures. The structural failure of Group A Hf-B compounds under shear

deformation was caused by the relatively weak hybridization interaction between Hf-B atoms, which led to the deformation of the 3-D boron network. It may be possible to obtain TM-B compounds with high mechanical properties through improving the hybridization interaction of TM-B atoms while maintaining a high B content when the designing a TM-B structure.

Acknowledgements

Declarations

Conflict of interest   There are no conflicts to declare.

Supplementary Information: The online version contains supplementary material available at http s://doi.org/10.1007/s10853-022-08022-w.

References

[1] Kaner RB, Gilman JJ, Tolbert SH (2005) Designing superhard materials. Science 308:1268–1269

[2] Bundy FP, Hall HT, Strong HM, Wentorf RH (1955) Man-made diamonds. Nature 176:51–55

[3] Tian Y, Xu B, Yu D et al (2013) Ultrahard nanotwinned cubic boron nitride. Nature 493:385–388

[4] Colinet C, Tedenac JC (2014) Enthalpies of Formation and electronic densities of states of vanadium borides. J Phase Equilib Diffus 35:396–405

[5] Kolmogorov AN, Shah S, Margine ER, Bialon AF, Hammerschmid TT, Drautz R (2010) New superconducting and semiconducting Fe-B compounds predicted with an ab initio evolutionary search. Physl Rev Lett 105:217003

[6] Li P, Zhou R, Zeng XC (2015) Computational analysis of stable hard structures in the Ti-B system. ACS Appl Mater Interfaces 7:15607–15617

[7] Xi-Yue C, Xing-Qiu C, Dian-Zhong L, Yi-Yi L (2014) Computational materials discovery: the case of the W-B system. Acta Crystallogr A 70:85–103

[8] Xu C, Bao K, Ma S, Ma Y, Wei S, Shao Z et al (2017) A first-principles investigation of a new hard multi-layered MnB_2 structure. RSC Adv 7:10559–10563

[9] Zhang M, Wang H, Wang H, Cui T, Ma Y (2010) Structural modifications and mechanical properties of molybdenum borides from first principles. J Phys Chem C 114:6722–6725

[10] Shein IR, Ivanovskii AL (2008) Elastic properties of mono- and polycrystalline hexagonal AlB2-like diborides of s, p and d metals from first-principles calculations. J Phys Condens Matter 20:8106–8110

[11] Vajeeston P, Ravindran P, Ravi C, Asokamani R (2001) Electronic structure, bonding, and ground-state properties of AlB_2-type transition-metal diborides. Phy Rev B 63:33–41

[12] Chung HY, Weinberger MB, Levine JB, Cumberland RW, Kavner A, Yang JM et al (2007) Synthesis of ultra-incompressible superhard rhenium diboride at ambient pressure. Science 318:436–439

[13] Huang B, Duan YH, Hu WC, Sun Y, Chen S (2015) Structural, anisotropic elastic and thermal properties of MB (M=Ti, Zr and Hf) monoborides. Ceram Int 41:6831–6843

[14] Miao N, Sa B, Zhou J, Sun Z (2011) Theoretical investigation on the transition-metal borides with TaB-type structure: a class of hard and refractory materials. Comput Mater Sci 50:1559–1566

[15] Pan Y, Lin Y (2015) The influence of B concentration on the structural stability and mechanical properties of Nb-B compounds. J Phys Chem C 119:23175–23183

[16] Levy O, Hart Gus LW, Curtarolo S (2010) Hafnium binary alloys from experiments and first principles. Acta Mater 58:2887–2897

[17] Gasch M, Johnson S, Marschall J (2008) Thermal conductivity characterization of hafnium diborides-based ultra-high-temperature ceramics. J Am Ceram Soc 91(5):1423–1432

[18] Fahrenholtz WG, Hilmas GE, Talmy IG et al (2007) Refractory diborides of zirconium and hafnium. J Am Ceram Soc 90(5):1347–1364

[19] Clougherty EV, Pober RL, Kaufman L (1968) Synthesis of oxidation resistant metal diboride composites. Proc Zoological Soc Lond 242:1077–1082

[20] Zhang J, Oganov AR, Li X et al (2017) Pressure-stabilized hafnium nitrides and their properties. Phys Rev B 95(2):020103

[21] Xie X, Wen M, Dong H, Long H, Zhang X, Wu F, Mu Z (2022) Semiconductors with a chiral crystal structure in group IVB transition metal pernitrides. Phys Chem Chem Phys 24(36):22046–22056

[22] Zeng Q, Peng J, Oganov AR et al (2013) Prediction of stable hafnium carbides: Stoichiometries, mechanical properties, and electronic structure. Phys Rev B: Condens Matter Mater Phys 88:214107

[23] Sun Y, Yang C, Lu Y et al (2020) Transformation of metallic polymer precursor into nanosized $HfTaC_2$ ceramics. Ceram Int 46(5):6022–6028

[24] Polyakov MN, Morstein M, Maeder X et al (2019) Microstructure-driven strengthening of TiB2 coatings

deposited by pulsed magnetron sputtering. Surf Coat Technol 368:88–96

[25] Fuger C, Schwartz B, Wojcik T et al (2020) Influence of Ta on the oxidation resistance of WB_2-z coatings. J Alloy Compd 864:158121–158129

[26] Rogl P, Potter PE (1988) A critical review and thermodynamic calculation of the binary system: hafnium-boron. Calphad 12:207–218

[27] Akopov G, Yeung MT, Turner CL, Li RL, Kaner RB (2016) Stabilization of HfB_{12} in $Y_{1-x}Hf_xB_{12}$ under ambient pressure. Inorg Chem 55:5051–5055

[28] Cannon JF, Farnsworth PB (1983) High pressure syntheses of ThB_{12} and HfB_{12}. J Less Common Met 92(2):359–368

[29] Novikov NP, Borovinskaya IP, Merzhanov AG (1974) Dependence of the composition of the products and the combustion rate in metal—boron systems on the ratio of the reagents. Combust Explos Shock Waves 10(2):175–178

[30] Pan Y, Huang H, Wang X et al (2015) Phase stability and mechanical properties of hafnium borides: a first-principles study. Comput Mater Sci 109:1–6

[31] Xu X, Fu K, Li L et al (2013) Dependence of the elastic properties of the early-transition-metal monoborides on their electronic structures: a density functional theory study. Physica B 419:105–111

[32] Huang LH, Zhao YR, Zhang GT et al (2019) Prediction of HfB_3 from first-principles calculations: crystal structures, stabilities, electronic properties and hardnesses. Mol Phys 117:547–556

[33] Zhang G, Gao R, Zhao Y, Bai T, Hu Y (2017) First-principles investigation on crystal structure and physical properties of HfB_4. J Alloy Compd 723:802–810

[34] Xie C, Zhang Q, Zakaryan HA et al (2019) Stable and hard hafnium borides: a first-principles study. J Appl Phys 125(20):205109

[35] Chu B, Li D, Bao K, Tian F, Duan D, Sha X et al (2014) Ultrahard boron-rich tantalum boride: monoclinic TaB_4. J Alloy Compd 617:660–664

[36] Latini A, Rau JV, Teghil R, Generosi A, Albertini VR (2010) Superhard properties of rhodium and iridium boride films. ACS Appl Mater Interfaces 2:581–587

[37] Levine JB, Tolbert SH, Kaner RB (2009) Advancements in the search for superhard ultra-incompressible metal borides. Adv Funct Mater 19:3519–3533

[38] Niu H, Wang J, Chen XQ, Li D, Li Y, Lazar P et al (2012) Structure, bonding, and possible superhardness of CrB_4. Phys Rev B 85:144116

[39] Pan Y, Wang X, Li S, Li Y, Wen M (2018) DFT prediction of a novel molybdenum tetraboride superhard material. RSC Adv 8:18008–18015

[40] Lyakhov AO, Oganov AR, Stokes HT, Qiang Z (2013) New developments in evolutionary structure prediction algorithm USPEX. Comput Phys Commun 184:1172–1182

[41] Oganov AR, Glass CW (2006) Crystal structure prediction using ab initio evolutionary techniques: principles and applications. J Chem Phys 124:201–419

[42] Oganov AR, Lyakhov AO, Valle M (2011) How Evolutionary Crystal Structure Prediction Works—and Why. Acc Chem Res 44:227–237

[43] Zhu Q, Oganov AR, Glass CW, Stokes HT (2012) Constrained evolutionary algorithm for structure prediction of molecular crystals: methodology and applications. Acta Crystallogr A 68:215–226

[44] Kresse G, Joubert D (1999) From ultrasoft pseudopotentials to the projector augmented-wave method. Phys Rev B 59:1758–1775

[45] Kresse G, Furthmüller J (1996) Efficient iterative schemes for ab initio total-energy calculations using a plane-wave basis set. Phys Rev B Condens Matter 54:11169–11186

[46] Perdew JP, Burke K, Ernzerhof M (1996) Generalized gradient approximation made simple. Phys Rev Lett 77:3865–3868

[47] Blöchl PE (1994) Projector augmented-wave method. Phys Rev B Condens Matter 50:17953–17979

[48] Page YL, Saxe P (2002) Symmetry-general least-squares extraction of elastic data for strained materials from ab initio calculations of stress. Phys Rev B 65:104104

[49] Yao HZ, Ouyang LZ, Ching WY (2007) Ab initio calculation of elastic constants of ceramic crystals. J Am Ceram Soc 90(10):3194–3204

[50] Cowley RA (1976) Acoustic phonon instabilities and structural phase transitions. Phys Rev B Condens Matter 13:4877–4885

[51] Chen XQ, Niu H, Li D, Li Y (2011) Modeling hardness of polycrystalline materials and bulk metallic glasses. Intermetallics 19:1275–1281

[52] Wei S, Da Y, Liu Z, Tian F, Duan D (2016) Strong covalent boron bonding induced extreme hardness of VB_3. J Alloy Compd 668:1101–1107

[53] Roundy D, Krenn CR, Cohen ML, Morris JW (1999) Ideal shear strengths of fcc aluminum and copper. Phys Rev Lett 82(13):2713–2716

[54] Dong H, Oganov AR, Zhu Q, Qian GR (2015) The phase diagram and hardness of carbon nitrides. Sci Rep 5(1):9870

[55] Wang K, Long G, Shang P (2018) Phonon dispersions, band structures, and dielectric functions of BeO and BeS polymorphs. J Phys Chem Solids 118:242–247

[56] Zhang X, Zeng Z, Cheng Y, Ji G (2016) Lattice dynamics, phonon vibrational spectra, and thermal properties of

tetragonal SrPt$_3$P: a first-principles study. RSC Adv 6(32):27060–27067

[57] Mouhat F, Coudert FOX (2014) Necessary and sufficient elastic stability conditions in various crystal systems. Phys Rev B 90(22):224104

[58] Yuan Y, Huang Y, Ma F et al (2017) Effects of oxygen vacancy on the mechanical, electronic and optical properties of monoclinic BiVO$_4$. J Mater Sci 52(14):8546–8555

[59] Kojima Y, Ohfuji H (2013) Structure and stability of carbon nitride under high pressure and high temperature up to 125 GPa and 3000 K. Diam Relat Mater 39(10):1–7

[60] Pugh SF (2009) XCII. Relations between the elastic moduli and the plastic properties of polycrystalline pure metals. Philos Mag 45:823–843

[61] Lawson JW, Bauschlicher CW Jr, Daw MS (2011) Ab initio computations of electronic, mechanical, and thermal properties of ZrB$_2$ and HfB$_2$. J Am Ceram Soc 94:3494–3499

[62] Hill R (1952) The elastic behaviour of a crystalline aggregate. Proc Phys Soc 65(5):349–354

[63] Zhang X, Luo X, Li J, Hu P, Han J (2010) The ideal strength of transition metal diborides TMB$_2$ (TM = Ti, Zr, Hf): plastic anisotropy and the role of prismatic slip. Scripta Mater 62(8):625–628

[64] Zhang M, Yan H, Zheng B, Wei Q (2015) Influences of carbon concentration on crystal structures and ideal strengths of B$_2$C$_x$O compounds in the B-C-O system. Sci Rep 5(1):15481

[65] Miao Z, Mingchun L, Yonghui D, Lili G, Cheng L, Hanyu L (2014) Hardness of FeB$_4$: density functional theory investigation. J Chem Phys 140(17):174505